Coherent Transients In 3-Level Systems: Quadrupoles, Quarks, and Quantum Beats

M. Mehring

Institut fur Physik
Universitat Dortmund
Dortmund, West Germany

I. INTRODUCTION

A 3-level system is comprised of three Hilbert states labeled |1>, |2>, and |3>. In general, these 3 states represent a subsystem of a more complex multilevel system in atoms, molecules, or solids. As soon as we connect two of these three states by some time dependent interaction, transients occur. Numerous experiments of this sort have been performed recently in optical (1-5) as well as in radio-frequency (RF) spectroscopy (6-14).

We shall restrict ourselves here to three simple objects like those sketched in Figure 1. To be more specific, let us consider the three energy levels of a spin $I = 1$ in a large magnetic field $H_o = \omega_o/\gamma$, where γ is the gyromagnetic ratio and ω_o is the Larmor frequency. In the case of a small quadrupolar interaction $\omega_Q << \omega_o$, the Hamiltonian which gives rise to energy level shifts in first order may be written as (15)

$$\mathcal{H}_o = -\omega_o I_z + \omega_Q [I_z^2 - I(I+1)/3] \qquad (1)$$

Figure 2 shows the corresponding energy level diagram for a spin $I = 1$. Allowed ($\delta m = 1$) and forbidden (double quantum $\delta m = 2$) transitions are indicated. Note that levels $|\pm 1\rangle$ are shifted by $+\frac{1}{3}$ and the level $|0\rangle$ is shifted by $-\frac{2}{3}$, in multiples of the quadrupolar interaction ω_Q.

|1>	|2>	|3>	Hilbert states
|+1>	|0>	|-1>	Spin-1 Eigenstates
u	s	d	Quarks
up	strange	down	Gell-Mann, Ne'eman

Figure 1. Three objects taken out of a manifold of states to represent 3-level systems.

Only two independent operators can be chosen to be diagonal, which we name, for reasons to become obvious later

$$\text{"isospin"} \qquad I_3 = I_z/2 \qquad (2)$$

and

$$\text{"hypercharge"} \qquad Y = I_z^2 - I(I+1)/3$$

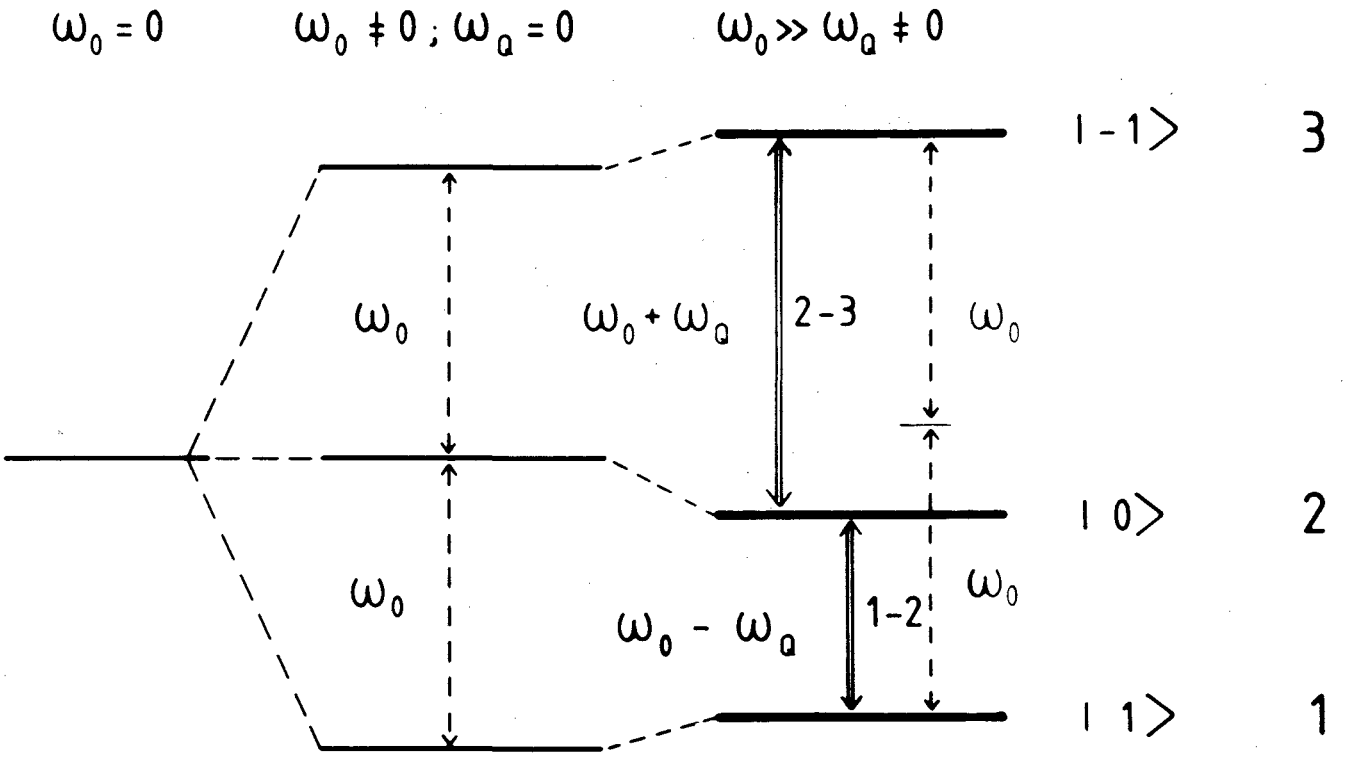

Figure 2. The 3-level system of a spin-1 with quadrupolar interaction ω_Q in a large magnetic field $\mathcal{H}_0 = \omega_0/\gamma$ with $\omega_0 >> \omega_Q$. Allowed ($\Delta m = 1$) and forbidden ($\Delta m = 2$) transitions are indicated.

This notation is simular to that used in elementary particle physics (16). In our case, the "isospin" represents the spin orientation in the Zeeman field, whereas the "hypercharge" is a measure of the quadrupolar interaction. The eigenvalues of these operators in the three states $|+1\rangle$, $|0\rangle$, and $|-1\rangle$ are plotted in the $I_3 - Y$ plane as shown in Figure 3.

The correspondence with the three-quark model is obvious (16,17). This analogy is further indicated in Table 1 where the relevant quantum numbers for the three quarks, *u* (up), *d* (down), and *s* (strange), are listed. The table also contains the quantum number $Q = I_3 + Y/2$ for the electric charge. Many elementary particles can be represented by product states of these three quarks, for example, mesons (qq) and baryons (qqq). A few of these are listed in Table 2 for convenience (16,17). The three-quark model has been recently extended to a six-quark model, and the experimental evidence for five of the six quarks is already convincing.

II. SIMPLE 2-LEVEL EXPERIMENTS

Standard spectroscopy usually deals with two levels at a time in a multi-level system. Transition rates—Fermi's golden rule—and transients—Feynman, Vernon, and Hellwarth (18)—can be easily formulated and have been applied extensively to a variety of spectroscopical observations.

Let us consider a few basic experiments which will be of importance in 3-level experiments later. The interaction causing the transitions between the two levels may be expressed by

$$\mathcal{H}_1(t) = -\gamma \hat{I} H_1(t) \qquad (3)$$

where the time dependence of the magnetic field $H_1(t)$ is assumed to be a periodic function of the transition frequency ω_0. Transformation into the "rotating frame" (15) (interaction representation) leads to a time-independent Hamiltonian

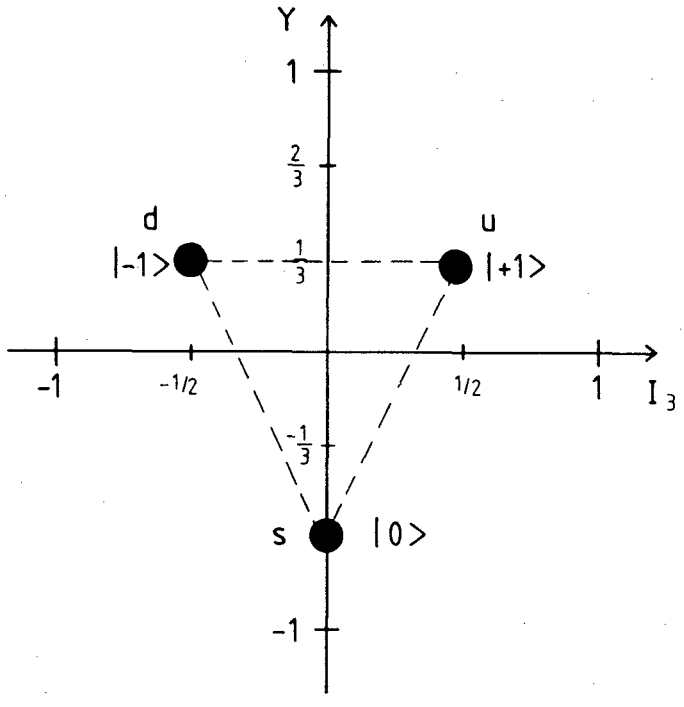

Figure 3. Hypercharge quantum number (Y) versus isospin quantum number (I_3) for different 3-level states according to Figure 1 and Table 1.

$$\mathcal{H}_1 = \omega_1 I_\alpha \qquad (\alpha = x, y, z) \tag{4}$$

where $\omega_1 = \gamma H_1$. In the following, we will always assume that transformation into the corresponding "rotating frame" has been performed.

The time dependence of the wave function $|\psi(t)\rangle$ may now be expressed by

$$|\psi(t)\rangle = e^{-i\beta(t)I_\alpha}|\psi(0)\rangle \tag{5}$$

where $\beta = \omega_1 t$ is the "rotation angle" during the "on time" of the field $H_1 = \omega_1/\gamma$. If special initial conditions and time reversal pulses are applied, standard transient effects like free induction decay (FID) and spin echos can be described.

Table 1. Analogy between Quarks q, Antiquarks q, and the States $|+1\rangle$, $|0\rangle$, and $|-1\rangle$ of a Spin $I = 1$. Charge $Q = I_3 + Y/2$.

State	Quarks q,q	Isospin I_3	Hypercharge Y	Charge Q
$\|+1\rangle$	μ,μ	$+\frac{1}{2},-\frac{1}{2}$	$+\frac{1}{3}$	$\frac{2}{3},-\frac{2}{3}$
$\|0\rangle$	s,s	0,0	$-\frac{2}{3}$	$-\frac{1}{3},+\frac{1}{3}$
$\|-1\rangle$	d,d	$-\frac{1}{2},+\frac{1}{2}$	$+\frac{1}{3}$	$-\frac{1}{3},+\frac{1}{3}$

Table 2. Quantum Numbers I_3, Y, and Q for Some Mesons and Baryons.

	Particle	Quarks	I_3 Y Q
Mesons	π^+	u d	+1 0 1
	π^0	d d u u	0 0 0
	π^-	d u	−1 0 −1
Baryons	proton	u u d	+½ 1 1
	neutron	u d d	−½ 1 0

We are interested here, however, in a special behavior, called "spinor behavior," of a two-level system. Let us suppose that we start at time $t = 0$ in the state $|1\rangle$ and apply a field $H_1 = \omega_1/\gamma$ for time t in the y-direction of the rotating frame; i.e., $\beta = \omega_1 t$. There will be a mixture of states $|1\rangle$ and $|2\rangle$ after time t as follows

$$|\psi(\beta)\rangle = \cos(\beta/2)|1\rangle + \sin(\beta/2)|2\rangle \tag{6}$$

Some observables, however, like the "polarization" $\langle\psi|P|\psi\rangle$, with $P|1\rangle = |1\rangle$ and $P|2\rangle = -|2\rangle$, will vary with β as

$$\langle\psi|P|\psi\rangle = \cos^2(\beta/2) - \sin^2(\beta/2) = \cos\beta \tag{7}$$

Table 3 lists the various states and polarization for different values of $\beta = n\pi$, $n = 0,1,2,3,4$. Note that the polarization is periodic with 2π, whereas the sign of the wave function is changed under 2π-rotation. This is stated as

$$\exp(-i2\pi\vec{I}\cdot\vec{n})|\psi\rangle = -|\psi\rangle \tag{8}$$

where $\vec{n}$ is the unit-vector of rotation and $|\psi|$ is a spinor, and holds for any two-level quantum system and also for fermions (half-integer spin). This

Table 3. Variation of the initial quantum state $|\psi\rangle = |1\rangle$ and of polarization $\langle\psi|P|\psi\rangle$ with the effective rotation angle β about an RF field applied in the y-direction of the $|1\rangle - |2\rangle$ rotating frame (see text).

β	$\|\psi\rangle$	$\langle\psi\|P\|\psi\rangle$
0	$\|1\rangle$	1
π	$\|2\rangle$	−1
2π	$-\|1\rangle$	1
3π	$-\|2\rangle$	−1
4π	$\|1\rangle$	1

behavior has been demonstrated in a number of molecular beam experiments (19), neutron beam interferometry (20,21), and what Stoll *et al* (8) have called NMR spin interferometric experiments.

Even in a spin-1 system, which is a boson rather than a fermion, spinor behavior can be demonstrated, as we have shown recently (12-14). In all these experiments, a reference state has to be present to permit measurement of the phase change of the "rotated" wave function. The minimum number of levels required for such an experiment is three. It is therefore not surprising that spinor behavior can be observed for a spin $I = 1$ (12-14).

III. SPINOR BEHAVIOR AND COHERENCE TRANSFER IN 3-LEVEL SYSTEMS

As noted in Section II, the phase change of a state under rotation can be observed only if a reference state with a constant phase is available. Consider an experiment where state $|1\rangle$ in the 3-level system in Figure 2 is used as a reference state and the phase of states $|2\rangle$ and $|3\rangle$ is rotated by 2π.

An experiment of this sort can be performed by first applying a $\pi/2$-pulse at the 1-2 transition to a system in state $|1\rangle$, which results in a superposition of states.

$$|\psi(0)\rangle = (|1\rangle + |2\rangle)/\sqrt{2} \qquad (9)$$

The corresponding magnetization (e.g., in the x-direction of the 1-2 rotating frame immediately after the pulse) is $\langle I_x^{1\text{-}2} \rangle = 1$. Secondly, let us apply radiation to the 2-3 transition, which will effectively rotate states $|2\rangle$ and $|3\rangle$ by an angle β, depending on the transition matrix elements and on time. After a 2π rotation, the wave function reads

$$|\psi(2\pi)\rangle = \exp(-2\pi I_y^{2\text{-}3})|\psi(0)\rangle = (|1\rangle + \cos\pi|2\rangle + \sin\pi|3\rangle)/\sqrt{2}$$

or

$$|\psi(2\pi)\rangle = (|1\rangle - |2\rangle)\sqrt{2} \qquad (10)$$

Consequently, the magnetization observed at the 1-2 transition will be inverted, i.e. $\langle I_x^{1\text{-}2} \rangle = -1$.

An experiment of this sort has been performed at the deuterium resonance in a single crystal of hexamethylbenzene (12). The resulting spin echo signal is shown in Figure 4 together with the pulse-timing. Moreover, it was demonstrated recently (13,14) that similar arguments hold for the double—quantum transition 1-3 ($\Delta m = 2$), and the same behavior can be observed, although the transition rates are of course reduced by the scaling factor ω_1/ω_Q (10).

The general behavior of the wavefunction under the above conditions can be expressed as

$$|\psi(\beta)\rangle = \{|1\rangle + \cos(\beta/2)|2\rangle + \sin(\beta/2)|3\rangle\}\sqrt{2} \qquad (11)$$

Such behavior was also observed in similar experiments performed with ^{27}Al ($I = 5/2$) in Al_2O_3 (6,7). Note that coherence transfer from state $|2\rangle$ to state $|3\rangle$ can be achieved if $\beta = \pi$. The wave function is now

$$|\psi(\pi)\rangle = \{|1\rangle + |3\rangle\}\sqrt{2} \qquad (12)$$

A two-step coherence transfer $[(\pi/2)^{1\text{-}2}; (\pi)^{2\text{-}3}]$ using allowed transitions ($\Delta m = 1$) results in the same coherence as a single $\pi/2$-pulse applied to the double-quantum ($\Delta m = 2$) transition (6,7). This coherence is not directly observable.

In a variation of this experiment, application of the π-pulse to the double-quantum 1-3 transition rather than to the allowed 2-3 transition establishes coherence between 2-3, i.e., a previously unobserved transient magnetization should be observable at the 2-3 transition. Figure 5 shows such an experiment in which phase-sensitive detection was used to demonstrate the phase relationship (14). The reference signal for the observed transient signal was generated by mixing the single-quantum RF (ω_{12}) with the double-quantum RF ($2\omega_o$) as follows

$$\omega_{23} = 2\omega_o - \omega_{12} \qquad (13)$$

Many experiments of this sort were invented. Among these is the second harmonic generation of Rabi oscillations and others (14).

A convenient way to explain these experiments is to use the fictitious spin $-\frac{1}{2}$ operators to describe the equation of motion of the density matrix (16,10,22,23). It has been shown recently (14) that in the case of spin-1 (3-level system) the spin motion can be described by equations of the form

$$\frac{d\vec{I}}{dt} = \vec{\Omega} \times \vec{I} \qquad (14)$$

where $\vec{I} = (I_a, I_b, I_c)$ is a fictitious spin vector in some reference frame, whereas $\vec{\Omega} = (\omega_a, \omega_b, \omega_c)$ is an effective field vector in the same frame. Three different types of reference frames can be distinguished (14), namely $\beta/2$-, β-, and 2β-rotational frames, where $\beta = |\vec{\Omega}| \cdot t$.

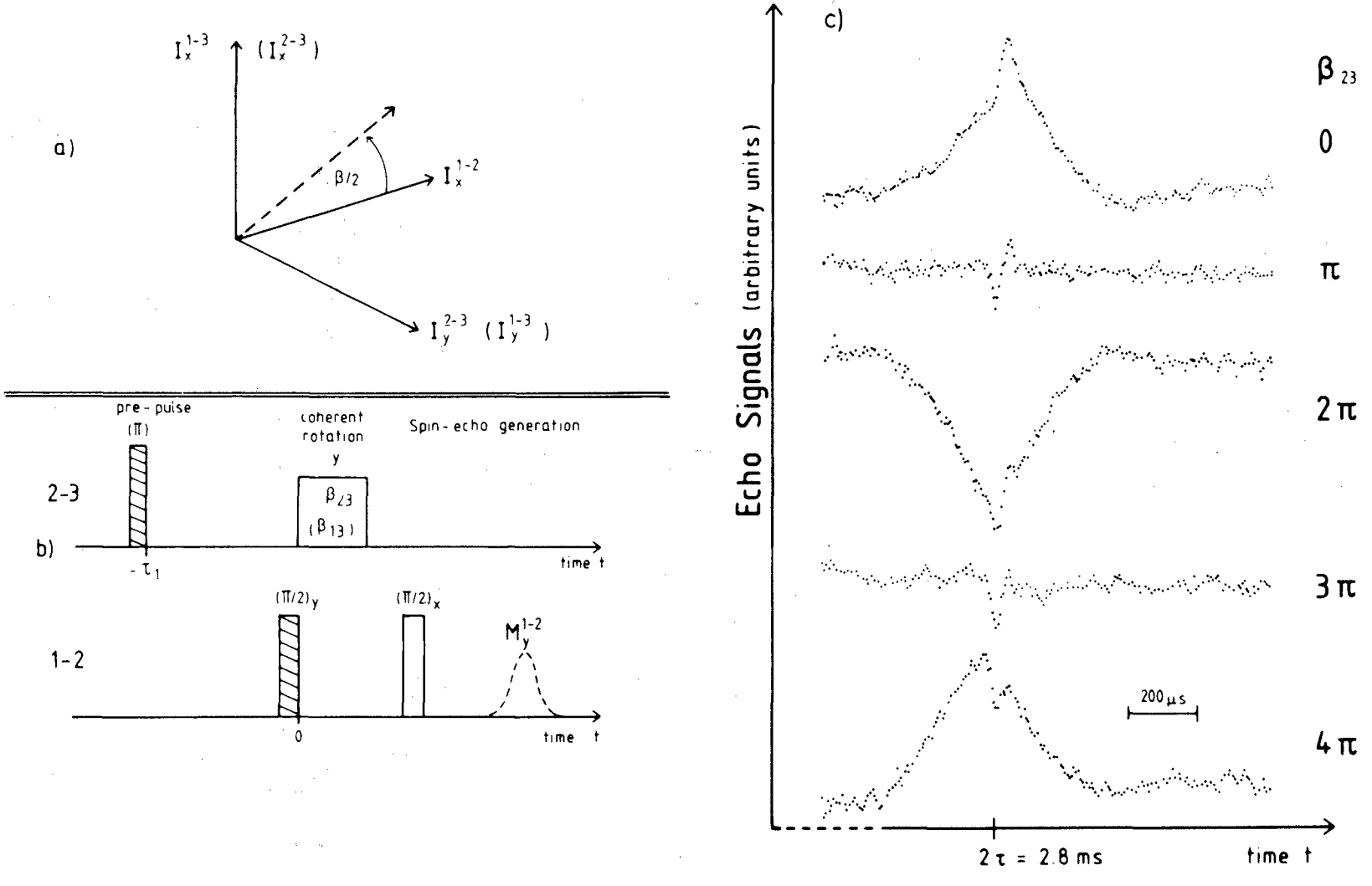

Figure 4. Pulse timing **(a)** and a fictitious spin-½ rotating frame for **(b)** a spinor experiment in a 3-level system. The observed spin echo signal, representing the 1-2 magnetization for different rotation angle $\beta 23$ of states |2> and |3> is shown in (c).

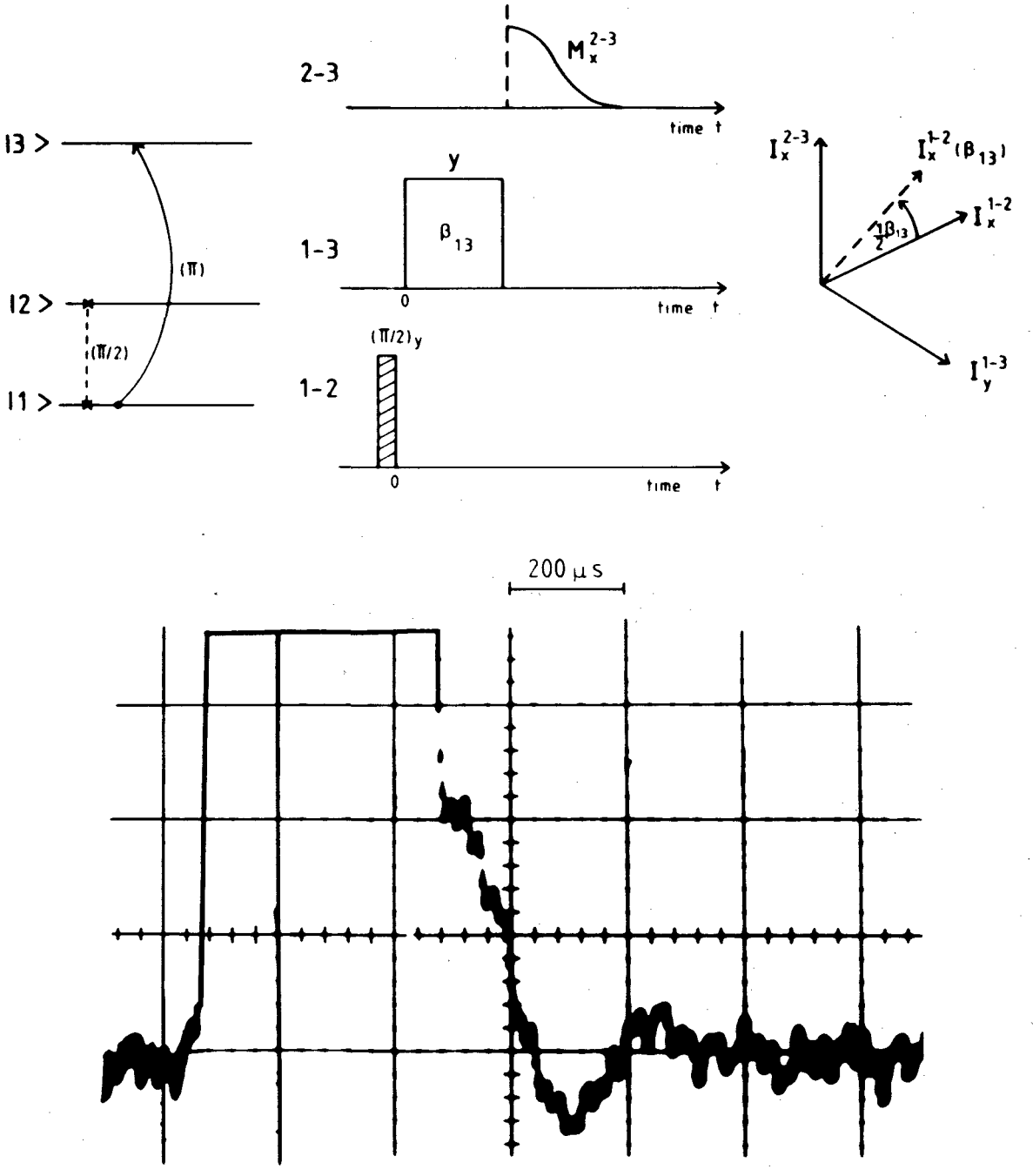

Figure 5. Pulse timing of a double quantum coherence transfer (top). The oscilloscope trace (bottom) shows the free induction decay FID excited at the 2-3 transition by irradiation only at the allowed (1-2) and the double-quantum (1-3) transition. Phase coherent detection of the FID is explained in the text.

IV. MULTIPLE FREQUENCY EXCITATION (MFE) OF A 3-LEVEL SYSTEM— SPECTROSCOPY OF QUADRUPOLAR BROADENED POWDER LINES

Time-resolved spectroscopy of quadrupolar broadened powder spectra of ^{14}N and ^{2}H nuclei is often difficult to perform because of the large spectral width involved. Technically, it would be difficult to excite a ^{14}N powder spectrum about 1 MHz wide with a single RF pulse. It might therefore be useful to consider a type of time-resolved spectroscopy of quadrupolar broadened spin-1 nuclei in a powder sample which uses the spin properties discussed above (24). One such sequence, for example, would use the double-quantum transition frequency ω_o which is unaffected by the quadrupolar interaction.

Here we restrict ourselves to the two allowed transitions labelled 1-2 and 2-3 in Figure 2. Both transitions will be excited simultaneously. This is equivalent to a rotation of the total nuclear spin. In other words, simultaneous irradiation at the two satellite transitions of a quadrupolar split line of a spin-1 corresponds to removing the quadrupolar interaction by transforming into the appropriate rotating frame. In a powder sample, of course, there are many satellite transitions distributed over a wide spectral range. This spectral range has to be covered by $2n + 1$ (n is an integer) independent spectrometers or by generating $2n$ sidebands and a central line from a single frequency source by a modulation technique. If the $2n + 1$ spectral lines are separated by frequency $\delta\omega$, the total spectral width covered is $\Delta\omega_{max} = 2n\delta\omega$.

Suppose all sidebands are created with the same initial phase once the RF pulse is started. A comb of sharply peaked pulses would result as the Fourier transform of the $2n + 1$ spectral lines. The power limitations of the transmitter would soon truncate such a sequence. In order to avoid interferometric enhancement of RF fields during MFE, all sidebands which are generated from a single coherent source have to be phased randomly. This can be achieved by amplitude modulation of the form (24)

$$\omega_1(t) = \omega_1 \sum_{j=1}^{n} \sin(j\delta\omega t + \zeta_j)$$

where the phases ζ_j are chosen randomly. The envelope of a typical MFE-pulse of this type is shown in Figure 6 together with the power spectrum of the emitted RF field. The necessary phase and frequency information can be stored in a digital memory and read out in the course of the applied pulse. In this way, a large flexibility concerning spectral width and frequency separation results. The following conditions have to be met:

$$\text{(i) } H_{1j} > H_L$$

where H_{1j} is the field strength of a single spectral line j and $H_L = \omega_L/\gamma$ is the "local field" causing homogeneous broadening,

$$\text{(ii) } \gamma H_{1j} << \delta\omega$$

to avoid interference effects between different spectral lines, and the MFE-pulse of duration t_p must have a spectral distribution such that

$$\text{(iii) } 2\pi/t_p << \delta\omega$$

Under these conditions and some other reasonable assumptions, the "power savings factor" $\eta = P_{SFE}/P_{MFE}$ can be estimated to be (24)

$$\eta = \Delta\omega_{max}/4\omega_L$$

Here P_{SFE} is the RF pulse power necessary to excite all the spins distributed among the total spectral width $\Delta\omega_{max}$ with a single pulse (roughly $\pi/2$-rotation), whereas P_{MFE} is the average power of a MFE-pulse.

As a typical example, let us consider a ^{2}H powder spectrum with $\Delta\omega_{max}/2\pi = 200$ kHz and $\omega_L/2\pi = 1$ kHz. The power savings factor is $\eta = 50$ in this case. This means that about 50 W instead of 2.5 kW of RF power is sufficient to excite the total power spectrum, as shown in Figure 7.

To facilitate a comparison between single-pulse excitation and MFE-spectroscopy, spectra obtained by both methods are shown in Figure 7. The MFE spectrum is, of course, multiline with an envelope which corresponds to the actual powder spectrum. The number of spectral lines has to be chosen according to the richness of the spectral information contained in the powder spectra. MFE spectroscopy will be specifically useful for ^{14}N studies because single-pulse excitation is not technically feasible for a spectral width larger than 1 MHz.

Finally, it should be noted that Mansfield and coworkers (26,27) have applied a similar type of MFE technique to spin imaging. Other fields of application

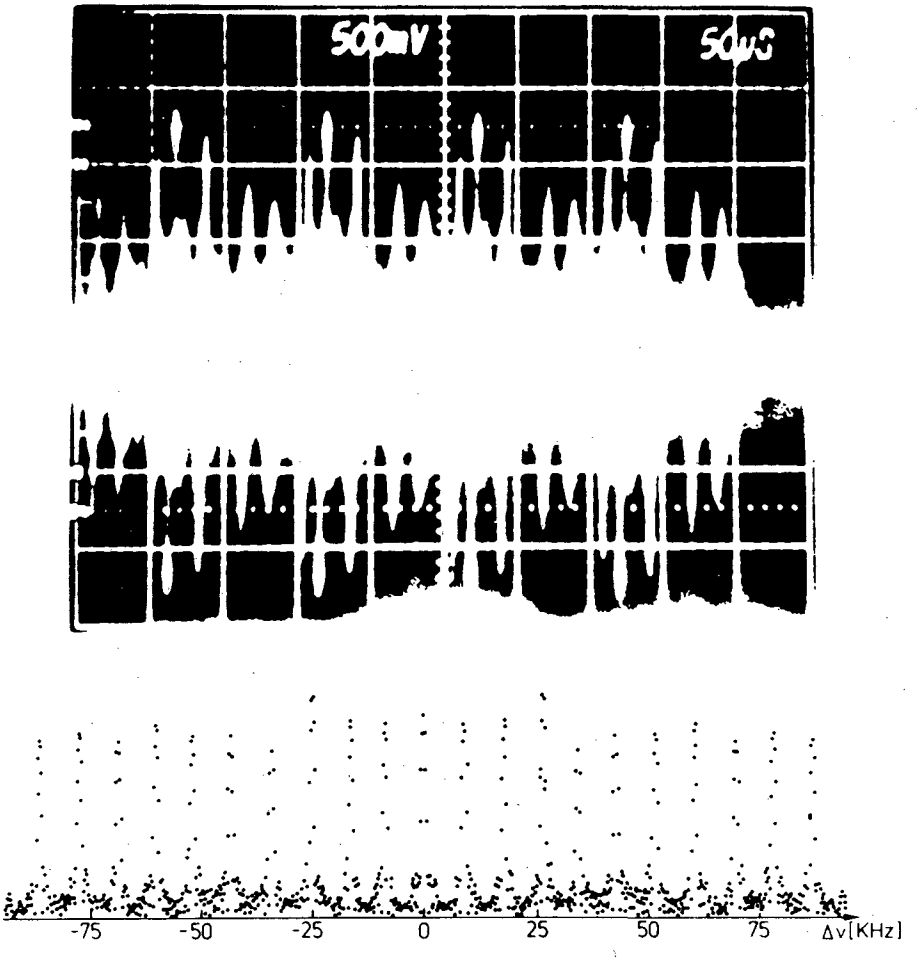

Figure 6. Envelope of a typical random phase MFE pulse together with its absolute value spectral representation, showing a multiline spectrum (24).

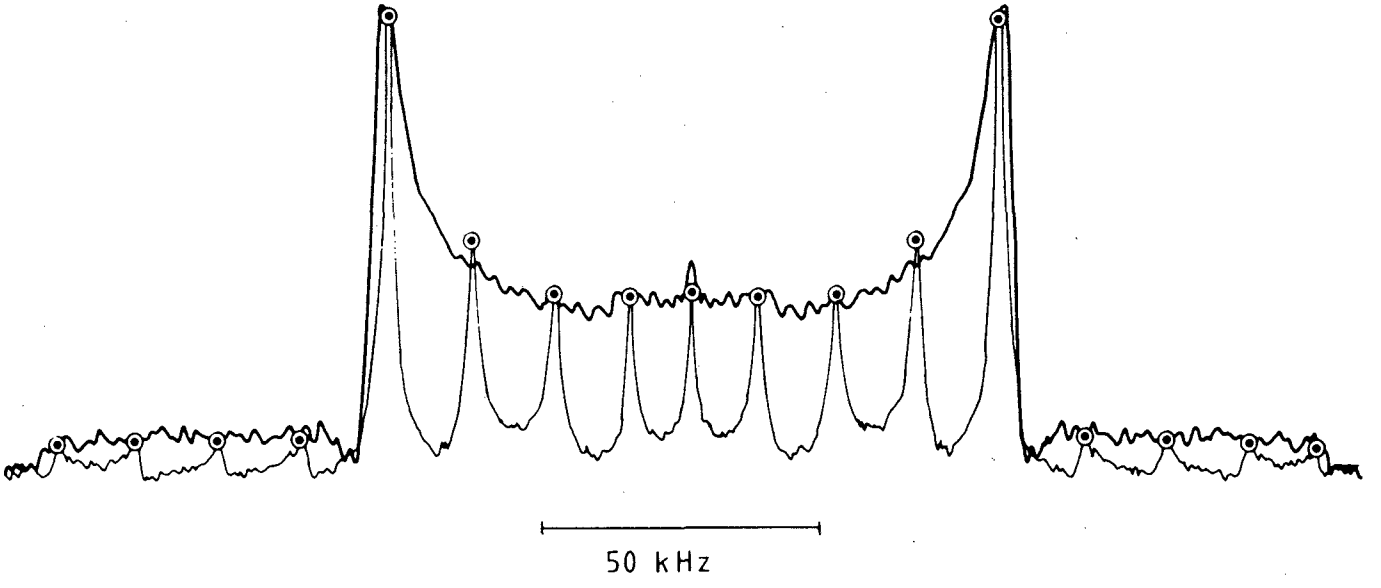

Figure 7. MFE-multiline spectrum in comparison with a single-pulse spectrum of deuterated polyethylene (24,25).

would be ESR and optical spectroscopy. Decoupling and saturation of broad lines as well as the investigation of relaxation phenomena over a wide spectral width become feasible with this technique.

In the case of the 3-level system (spin $I = 1$) discussed here, all experiments such as observation of spinor behavior and coherence transfer can be performed on powder samples with the MFE technique. Moreover, the MFE technique allows cross-polarization, for example, of rare ^2H and abundant ^1H in partially deuterated powder samples (24).

ACKNOWLEDGMENTS

I gratefully acknowledge enlightening discussions with Prof. R. Vaughan, Dr. M.E. Stoll, and Prof. A. Pines. Drs. D. Wemmer and E.K. Wolff performed most of the experiments, and Prof. H.W. Spiess kindly supplied the sample of deuterated polyformaldehyde. The work was supported in part by a financial contribution from the Deutsche Forschungsgemeinschaft (DFG).

REFERENCES

[1]R.G. Brewer and E.L. Hahn, *Phys. Rev. A* **11**, 1641 (1975).
[2]D. Grischkowsky, M.M.T. Loy, and P.F. Liao, *Phys. Rev. A* **12**, 2514 (1975).
[3]A. Flusberg and S.R. Hartmann, *Phys. Rev. A* **14**, 813 (1976).
[4]M.M.T. Loy, *Phys. Rev. Lett.* **36**, 5624 (1977).
[5]D. Grischkowsky and R.G. Brewer, *Phys. Rev. A* **15**, 1789 (1977).
[6]H. Hatanaka, T. Terao, and T. Hashi, *J. Phys. Soc. Jap.* **39**, 835 (1975).
[7]H. Hatanaka and T. Hashi, *J. Phys. Soc. Jap.* **39**, 1139 (1975).
[8]M.E. Stoll, A. Vega, and R.W. Vaughan, *Phys. Rev. A* **16**, 1521 (1977).
[9]A. Pines, D.J. Ruben, S. Vega, and M. Mehring, *Phys. Rev. Lett.* **36**, 110 (1976).
[10]S. Vega and A. Pines, *J. Chem. Phys.* **66**, 5624 (1977).
[11]D.G. Gold and E.L. Hahn, *Phys. Rev. A* **16**, 324 (1977).
[12]M.E. Stoll, E.K. Wolff, and M. Mehring, *Phys. Rev. A* **17**, 1561 (1978).
[13]E.K. Wolff and M. Mehring, *Phys. Lett.* **20A**, 125 (1979).
[14]M. Mehring, E.K. Wolff, and M.E. Stoll, *J. Magn. Reson.* **37**, 475 (1980).
[15]A. Abragam, *The Principles of Nuclear Magnetism*, Oxford University Press, London, 1961.
[16]S. Gasiorowicz, *Elementary Particle Physics*, Wiley, New York, 1967.
[17]M. Gell-Mann and U. Ne'eman, *The Eightfold Way*, W. A. Benjamin, New York, 1964.
[18]R.P. Feynman, F.L. Vernon, and R.W. Hellwarth, *J. Appl. Phys.* **28**, 49 (1957).

[19]E. Klempt, *Phys. Rev. D* **13**, 3125 (1975).
[20]H. Rauch, A. Zeilinger, G. Badurek, A. Wilfing, W. Bauspiess, and U. Bonse, *Phys. Lett.* **54A**, 425 (1975).
[21]S.A. Werner, R. Colella, A.W. Overhauser, and C.F. Eagan, *Phys. Rev. Lett.* **35**, 1053 (1975).
[22]S. Vega, *J. Chem. Phys.* **67**, 1752 (1977).
[23]A. Wokaun and R.R. Ernst, *J. Chem. Phys.* **67**, 1752 (1977).
[24]D.E. Wemmer, E.K. Wolff, and M. Mehring, *J. Magn. Reson.* **42**, 460 (1981).
[25]R. Hentschel and H.W. Spiess, *J. Magn. Reson.* **35**, 157 (1979).
[26]P. Mansfield and A.A. Maudsley, *J. Magn. Reson.* **27**, 101 (1977).
[27]P. Mansfield, A.A. Maudsley, and T. Baines, *J. Phys. E: Sci. Instr.* **6**, 271 (1976).